CHEMICAL ENGINEERING TRANSACTIONS
VOL. 84, 2021
A publication of AIDIC
The Italian Association of Chemical Engineering
Online at www.cetjournal.it
Guest Editors: Paolo Ciambelli, Luca Di Palma

ISBN 978-88-95608-82-2; **ISSN** 2283-9216
DOI: 10.3303/CET2184002

Facile Synthesis and Characterisation of Nanosized ZnO Modified with Ag_2S for Visible-light-induced Phenol Degradation

Emmanuel O. Ichipi*, Shepherd M. Tichapondwa, Evans M. N. Chirwa

Water Utilisation and Environmental Engineering Division, Department of Chemical Engineering, University of Pretoria, Pretoria 0002.
emmanuel.ichipi91@gmail.com

This study investigates the synthesis, characterisation, and application of a visible-light activated binary nanocomposite catalyst for the degradation of phenol in water. Zinc oxide with a wide direct band gap (3.4 eV) is efficient under ultraviolet irradiation but shows less activity under visible light. Therefore, a sol-gel method was applied to modify it using silver sulphide whose band gap is much lower (1.1 eV) to shift the photosensitivity of the composite catalyst towards the visible light spectrum. The synthesised nanoparticles were characterised using scanning electron microscopy, transmission electron microscopy, and X-ray diffraction which confirmed the purity of the synthesised material. At a catalyst loading of 1 gL^{-1}, results showed that under visible light, the binary composite Ag_2S/ZnO exhibited the highest phenol degradation efficiency of 50 % which was greater than ZnO that recorded a 16 % removal after 210 minutes of irradiation. These results support further development and application of visible-light-induced catalysts for photocatalytic degradation.

1. Introduction

With the continuous growth in technology development and industrialisation, pollutants such as phenolic compounds gradually find their way into the aquatic environment by spillage or leakages which results in serious damage overtime (Li et al., 2019). Phenol is one of the most common pollutants from the petroleum and plastics industry whose toxicity even at low concentrations has adverse effects to human health and damage aquatic life (Bruce et al., 1987). It is therefore essential that phenolic compounds be removed from wastewater before discharging it to the environs. Due to its obstinate and persistent nature in water, orthodox wastewater treatment techniques such as distillation and extraction are not effective to remove low concentration phenol from water (Villegas et al., 2016). Biodegradation using pure/mixed cultures is one of the environmentally friendly process of removing phenol from water, however, the microbes may not be efficacious in hypersaline systems application (Li et al., 2019). In the early 1980s, Advanced Oxidation Processes (AOPs) were first introduced to treat drinking water only (Deng and Zhao, 2015). Later on, AOPs were further developed and applied in many other treatment purposes since they utilize hydroxyl or sulfate radicals as major oxidant to degrade recalcitrant organic pollutants from wastewater (Deng and Zhao, 2015). Titanium and Zinc based photocatalysts are the most used due to their high chemical stability, low quantum yields, and cost (Nguyen et al., 2017). However, there are some limitations such as low visible light absorption abilities, high electron holes recombination, and high bandgap energy requirements which makes them only suitable for ultraviolet light (UV) irradiation therefore, more energy is required to initiate a charge carrier separation (Micheal et al. 2019). The solar spectrum that reaches the earth's surface consists of approximately 4 % UV light with the balance being 43 % of visible light and 53 % infrared, as a result, such catalyst will not be able to induce visible light (Samadi et al., 2016). Therefore, if the photosensitivity of the catalyst can be shifted towards the visible light region, it would greatly improve its degradation activity. Ongoing studies to modify photocatalysts include the introduction of dopants on the surface of the primary catalyst which in turn increases the dipole moment to change the electron transfer kinetics (Yin et al., 2019).

Paper Received: 26 May 2020; Revised: 11 October 2020; Accepted: 25 February 2021
Please cite this article as: Ichipi E., Tichapondwa S., Chirwa E., 2021, Facile Synthesis and Characterisation of Nanosized Zno Modified with Ag2s for Visible-light Induced Phenol Degradation, Chemical Engineering Transactions, 84, 7-12 DOI:10.3303/CET2184002

The layered structure of the primary catalyst creates adequate room for the atoms and orbitals to be polarized, hence there is effective separation and reduced recombination rates of the generated electron hole pairs (Adenuga et al., 2019).

Zinc oxide (ZnO) is a promising n-type semiconductor that has a direct wide band gap of about 3.37 eV and an excitation binding energy of approximately 60 meV at room temperature (Samadi et al., 2016). ZnO particles have a high surface area to volume ratio that creates more active sites for photocatalytic degradation, although they differ in structure based on the growth conditions during synthesis (Amornpitoksuk et al., 2012). Variant morphologies such as nano – rods, tubes pellets, or snowflakes and flower-like shapes depending on the method of preparation (Sun et al., 2016). Also, the preparation methods play a huge role in the particle's bandgap value, surface area, particle size, spatial structure and degradation potential (Faisal et al., 2015). The photodegradation efficiency of ZnO under visible light requires narrowing of the band gap and this can be achieved by metal or non-metal doping (Samadi et al., 2016). In the n-type doping of ZnO, atoms are replaced with one or more electrons in the outer shell to produce highly conductive particles (Klingshirn, 2007). Different narrow bandgap semiconductors have been investigated as dopants on ZnO in order to increase its effectiveness in the visible light spectrum, such includes CdS, CdSe, SnO, SnO_2, Ag_2S, PbS, GaAs, CuO, WO_3, and graphene (Johar et al., 2015). Silver sulphide (Ag_2S) with a direct band gap of approximately 1.1 eV and a relatively high absorption coefficient (104 m^{-1} cm^{-1}) at room temperature, can be photoexcited under visible light (Zhang et al., 2016). Therefore, a heterogeneous combination of Ag_2S and ZnO might develop an effective visible-light-driven photocatalyst that will achieve a longer charge carrier separation by suppressing the recombination of electron-holes, thus the photocatalytic efficiency is improved (Zhang et al., 2016).

In this research study, a binary Ag_2S/ZnO nanocomposite photocatalyst was synthesised via a sol-gel method and its degradation efficiency was tested on phenol polluted water under a simulated visible light environment. The samples were characterised using a field emission gun scanning electron microscopy (SEM) to confirm its morphology, shape, and size and a transmission electron microscopy (TEM) to measure the crystallite size and lattice fringe. X-ray diffraction (XRD) was also conducted to verify the crystallographic structure, chemical composition, and physical properties of the materials.

2. Materials and methods

2.1 Chemical and reagents

Zinc acetate (Zn $(CH_3COO)_2.2H_2O$), Urea (CO $(NH_2)_2$) sodium sulphide (Na_2S), and silver nitrate ($AgNO_3$) were purchased from Glassworld (Johannesburg, South Africa). Phenol (the organic pollutant), methanol, ethanol, acetic acid, and acetonitrile for HPLC use were purchased from Merck, South Africa. All these chemicals and reagents were used as obtained; no further purification was done before use. Distilled water was used during the experiment.

2.2 Catalyst synthesis

The synthesis technique of binary Ag_2S/ZnO nanocomposite was amended from a previous reported method by Marinho et al. (2012). ZnO precursor was prepared by dissolving 4.46 g of Zn $(CH_3COO)_2.2H_2O$ and 1.80 g of CO $(NH_2)_2$ in 50 ml of distilled water. The mixture was placed in an autoclave at 120 °C for 2 h and a white precipitate was formed. The precipitate was washed with distilled water and ethanol 3 times each before it was dried in the oven to form the ZnO precursor. The precursor powder was calcined in a furnace at a temperature of 500 °C for 3 h to remove all the volatile substances and pure ZnO was formed. The binary composite Ag_2S/ZnO was prepared by dissolving 1 g of pure ZnO in a 100 ml solution of 60/40 % v/v methanol and distilled water. 0.16 g of $AgNO_3$ was added to the solution and sonicated for 40 min to agitate the particle mixture. Finally, 0.06 g of Na_2S was added with continuous stirring for 8 h. The precipitate was washed with distilled water and ethanol several times, each time it was centrifuged at high speed. The resultant powder was collected and dried at 70 °C for 12 h. The procedure was done in dark to avoid surface plasmon resonance of the Ag constituent, however, a change in color was observed upon the addition of silver and sodium sulphide as seen in Figure 1 (a) and (b) (Ao et al., 2014).

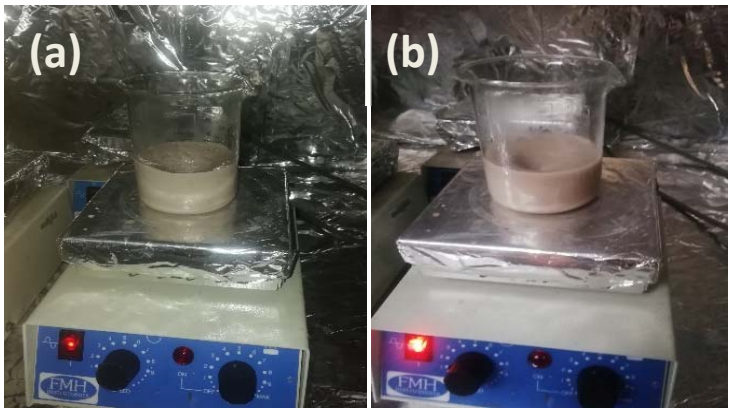

Figure 1: (a) ZnO before and (b) and after the addition of Ag_2S during synthesis in dark

2.3 Analytical methods

The SEM images were taken on a Zeiss Ultra PLUS FEG SEM and the TEM pictures on a JOEL JEM 2100F TEM. XRD analysis was carried out using a PANalytical X'Pert Pro powder diffractometer in θ–θ configuration with an X'Celerator detector, a variable divergence and fixed receiving slits with Fe filtered Co-Kα radiation (ʎ =1.789 Å). The crystallography of the materials was obtained by selecting the best–fitting pattern from the ICSD database to the measured diffraction pattern, using X'Pert Highscore plus software.

2.4 Photocatalytic activity

The photocatalytic activities of ZnO and binary Ag_2S/ZnO composite were investigated by tracking the photodegradation of phenol in water assisted by UV and visible light irradiation. The experimental set-up consisted of a box equipped with a 40 W actinic black light during the UV exposure experiment and was changed to three 18 W fluorescent day light lamps for the visible light experiments. All the tests were performed on 10 mgL^{-1} phenol concentration at a 100 ml volume using 1 gL^{-1} of catalyst loading. The reactor contents were placed on a stirrer for 30 minutes in the dark to allow for absorption-desorption equilibrium before the lights were switched on. 2 ml samples were collected at every 30 min interval from the reactor and subsequently centrifuged at 9,000 rpm for 10 minutes. Upon separation, the liquid was withdrawn using a syringe and filtered using a simplepure 0.45 µm into vial sample bottles. The samples were then analysed using a High-Performance Liquid Chromatography (HPLC – waters 2695 separation module, 2996 Photodiode Array detector), with Empower software. The parameters for detection of phenol were PAH C18 (4.6 x 250 mm, 5 µm) column, injection volume of 10 µL, a flow rate of 1.0 $mLmin^{-1}$, a wavelength of 280 nm, and a mobile phase of 1 % acetic acid in water and acetonitrile at 50 % each. The total degradation achieved after 3.5 h was determined given the expression below.

$$\% \text{ Degradation} = \frac{(C_0 - C_t)}{C_0} \times 100 \quad (1)$$

where C_0 (mg/L) is the initial concentration of phenol and C_t (mg/L) is the concentration of phenol at any given time, t.

3. Results and discussion

3.1 Characterisation of the catalyst

X-ray Diffraction analysis

The diffraction peaks and patterns of the synthesised ZnO precursor, pure ZnO, and Ag_2S/ZnO particles are shown in Figure 2. The strong, sharp, and narrow peaks show the high level of crystallinity of the materials. The peaks of pure ZnO depict the hexagonal crystal standard which belongs to the wurtzite-type ZnO called zincite (Dac Dien, 2019). The percentage composition of Ag_2S in the binary composite was relatively small hence, Ag_2S/ZnO and ZnO had identical reoccurring characteristic peaks, which implies the high purity of the synthesised catalysts.

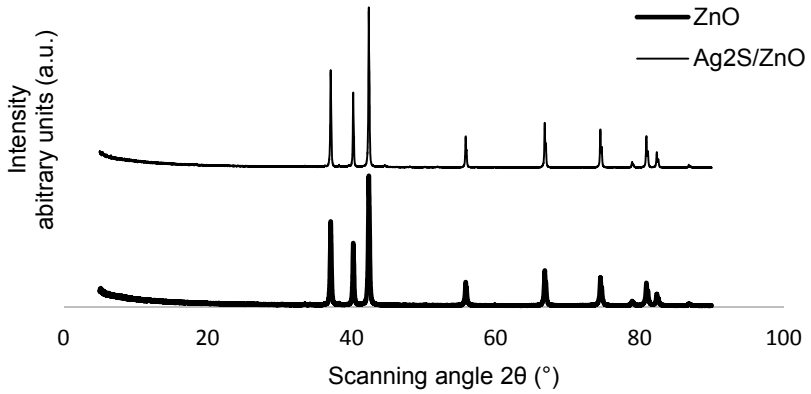

Figure 2: XRD pattern of ZnO and Ag_2S/ZnO catalysts synthesised by sol-gel method

SEM and TEM images

Some quantities of ZnO precursor, pure ZnO, and Ag_2S/ZnO powders were taken to SEM and TEM to capture their shapes and morphologies. Figure 3(a) shows the SEM image of precursor zinc oxide that looks like nanoflakes with spikes. Figure 3(b) reveals the formation of pure ZnO in a different morphology like spherical nanoparticles due to the calcination temperature. In Figure 3(c) the binary Ag_2S/ZnO resembles a mix of microrods and spherical-like particles which resembles the morphology of pure ZnO as described by Dac Dien (2019). Figures 3(d), (e), and (f) show TEM images of precursor ZnO, pure ZnO, and Ag_2S/ZnO particles like flat nanoplates and sheets.

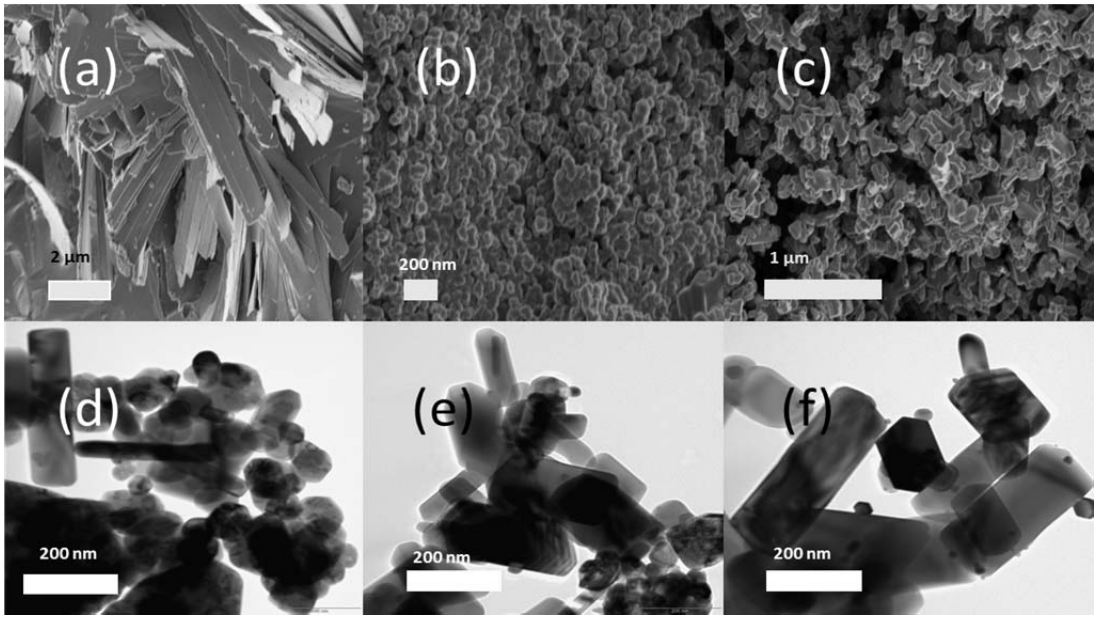

Figure 3: SEM image of (a) precursor ZnO. (b) pure ZnO. (c) Ag_2S/ZnO. TEM image of (d) precursor ZnO. (e) Pure ZnO. (f) Ag_2S/ZnO

3.2 Degradation studies

The photocatalytic degradation of phenol as a function of irradiation times on ZnO and Ag_2S/ZnO powders are shown in Figures 4 and 5. The photolysis test (without catalyst) degraded 4 % of phenol which shows that there is very little or no bond cleavage based on light exposure only. The photolysis test was done with the aid

of visible light setup which is in line with the scope of this study. A catalysis experiment (adsorption) that was carried out on both catalysts showed that ZnO and Ag_2S/ZnO had 18 % and 14 % degradation in 3.5 h respectively as shown in Figure 4. This can be attributed to the adsorption-desorption equilibrium of the phenol compounds to the surface of the semiconductor catalysts in the dark.

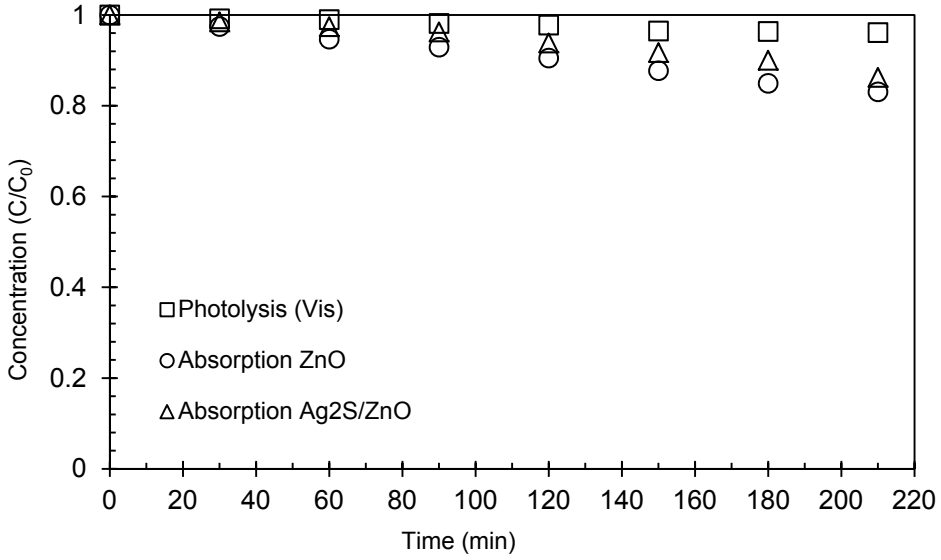

Figure 4: Graphical illustration of photolysis and adsorption test for both catalysts.

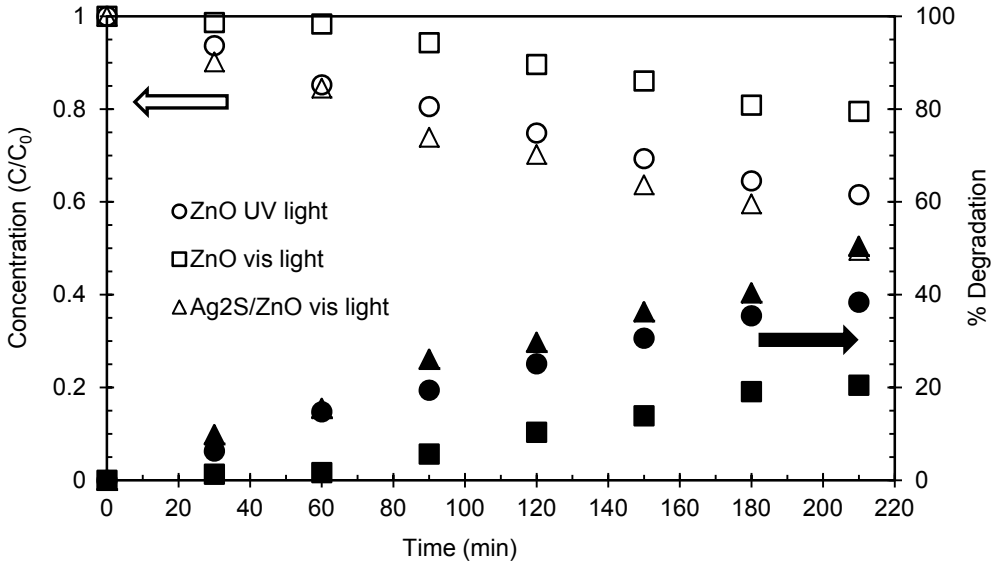

Figure 5: Photodegradation of phenol under UV and visible light irradiation.

Figure 5 showed a better performance of ZnO at 38 % under UV irradiation than visible light that could only degrade 16 %. As expected, results show that the main catalyst, Ag_2S/ZnO had the highest degradation by 50 % under visible light in 3.5 h. Further exposure for 24 h resulted in no traces of phenol depicting that the catalyst is able to completely degrade the pollutant at a longer period of time.

4. Conclusions

ZnO semiconductor photocatalyst like many other wide bandgap semiconductors is more effective under UV irradiation than visible light. Hence it was modified using Ag_2S to shift its photosensitivity towards the visible light spectrum. The SEM and TEM analysis of the synthesised composites confirms its microrod and nanoplate-like morphology. The XRD peak patterns show the presence of the individual constituent and purity of the nanocomposites. This study showed that ZnO can be modified using Ag_2S as a dopant and be a potential catalyst for the photodegradation of phenol in water under visible light irradiation.

References

Adenuga D., Tichapondwa S., Chirwa E., 2019, Synthesis and characterisation of potential visible-light photocatalyst and its photocatalytic activity in the decomposition of phenol, Chemical Engineering Transactions, 74**,** 1087.

Ao Y., Tang H., Wang P., Wang, C., 2014, Deposition Of Ag@AgCl onto two Dimensional square-like BiOCl nanoplates for high visible-light photocatalytic activity, Materials Letters, 131**,** 74-77.

Amornpitoksuk P., Suwanboon S., Sangkanu S., Sukhoom A., Muensit N., Baltrusaitis J., 2012, Synthesis, Characterization, Photocatalytic and Antibacterial Activities of Ag-Doped ZnO powders modified with a diblock copolymer, Powder Technology, 219**,** 158-164.

Bruce R. M., Santodonato J., Neal, M. W., 1987, Summary review of the health effects associated with phenol, Toxicol Ind Health, 3**,** 535-68.

Dac Dien N., 2019, Preparation of various morphologies of ZnO nanostructure through wet chemical methods, Advanced Material Science, 4.

Deng Y., Zhao R., 2015, Advanced Oxidation Processes (AOPs) in wastewater treatment, Current Pollution Reports, 1**,** 167-176.

Faisal M., Ibrahim A. A., Harraz F. A., Bouzid H., Al-Assiri M. S., Ismail A. A., 2015, SnO_2 doped ZnO nanostructures for highly efficient photocatalyst, Journal Of Molecular Catalysis A: Chemical, 397**,** 19-25.

Johar M. A., Afzal R. A., Alazba A. A., Manzoor U., 2015, Photocatalysis and bandgap engineering using ZnO nanocomposites, Advances In Materials Science and Engineering, 2015**,** 1-22.

Klingshirn C, 2007, ZnO: From basics towards applications, Physica Status Solidi (B), 244**,** 3027-3073.

Li H., Meng F., Duan W., Lin Y., Zheng Y., 2019, Biodegradation of phenol in saline or hypersaline environments by bacteria: A Review. Ecotoxicol Environ Saf, 184**,** 109658.

Marinho J. Z., Romeiro F. C., Lemos S. C. S., Motta F. V., Riccardi C. S., Li M. S., Longo E., Lima R. C., 2012, Urea-Based synthesis of Zinc oxide nanostructures at low temperature, Journal Of Nanomaterials, 2012**,** 1-7.

Nguyen T. V., Dao P. H., Duong K. L., Duong Q. H., Vu Q. T., Nguyen A. H., Mac V. P., Le T. L., 2017, Effect of R-TiO_2 and ZnO nanoparticles on the UV-shielding efficiency of Water-Borne Acrylic coating, Progress in Organic Coatings, 110**,** 114-121.

Samadi M., Zirak M., Naseri A., Khorashadizade E., Moshfegh A. Z., 2016, Recent progress on doped ZnO nanostructures for visible-light photocatalysis, Thin Solid Films, 605**,** 2-19.

Sun Y., Chen L., Bao Y., Zhang Y., Wang J., Fu M., Wu J., Ye D., 2016, The Applications of morphology controlled ZnO in catalysis, Catalysts, 6**,** 188.

Villegas L., Mashhadi N., Chen M., Mukherjee D., Taylor K., Biswas N., 2016, A Short review of techniques for phenol removal from wastewater, Current Pollution Reports, 2.

Yin W., Wen B., Ge Q., Zou D., Xu Y., Liu M., Wei X., Chen M. & Fan X., 2019, Role of Intrinsic dipole on photocatalytic water splitting for Janus Mosse/Nitrides heterostructure: A First-Principles study, Progress in Natural Science: Materials International, 29**,** 335-340.

Zhang X., Liu X., Zhang L., Li D, Liu S., 2016, Novel Porous Ag_2S/ZnS composite nanospheres: Fabrication and enhanced visible-light photocatalytic activities, Journal of Alloys and Compounds, 655, 38-43.